G&G

Gem News International

Contributing Editors

Emmanuel Fritsch, *University of Nantes, CNRS, Team 6502, Institut des Matériaux Jean Rouxel (IMN), Nantes, France* (fritsch@cnrs imn.fr)

Gagan Choudhary, *Gem Testing Laboratory, Jaipur, India* (gagan@gjepcindia.com)

Christopher M. Breeding, *GIA, Carlsbad* (christopher.breeding@gia.edu)

COLORED STONES AND ORGANIC MATERIALS

Kämmererite cabochons from India. Kämmererite is a purple variety of clinochlore, a mica-like Mg-Al-silicate with the formula $(Mg,Fe)_5Al[(OH)_8|AlSi_3O_{10}]$. Its color is caused by chromium. Kämmererite is always found in fractures of ultrabasic rocks, usually with chromite ore. The only known locality for transparent crystals is the Kop Krom chromite mine in the Kop Daglari Mountains of Turkey. Transparent crystals from this area (figure 1) can measure up to 2 cm. Some of this material has been faceted as rare collector gemstones (H. Bank and H. Rodewald, "Schleifwürdiger, roter, durchsichtiger Chlorit: Kämmererit," *Zeitschrift der Deutschen Gemmologischen Gesellschaft*, Vol. 28, No. 1, 1979, 39–40, in German).

An unknown location in India recently yielded massive kämmererite that was used to carve interesting cabochons (figure 2); 10 such samples were examined in this study. The cabochons have an attractive light to dark purple color; some thinner pieces are translucent. Some of the material shows a folded texture, and this type is visually similar to charoite, a well-known ornamental stone from Siberia. The measured refractive index (RI) of the new kämmererite is approximately 1.57, very close to charoite, but clinochlore has a much lower Mohs hardness (about 2.5, rather than charoite's 5–6). This new kämmererite is inert under UV light, but white layers in the samples show creamy fluorescence under both long-wave and short-wave UV. Raman spectroscopy revealed a characteristic group of peaks at 3877, 4063, 4175, 4500, and 4920 cm^{-1} in the spectrum (figure 3), confirming the material's identity. Visible spectra further supported this conclusion. The amount of

Figure 1. This 57 mm wide kämmererite rough and 0.57 ct faceted stone are from the Kop Daglari Mountains of Turkey. Photo by Jaroslav Hyršl.

Figure 2. These kämmererite cabochons, with widths of 27 mm and 21 mm, are from an undisclosed location in India. Photo by Jaroslav Hyršl.

Editors' note: Interested contributors should send information and illustrations to Stuart Overlin at soverlin@gia.edu or GIA, The Robert Mouawad Campus, 5345 Armada Drive, Carlsbad, CA 92008.

Gems & Gemology, Vol. 52, No. 2, pp. 206–220.

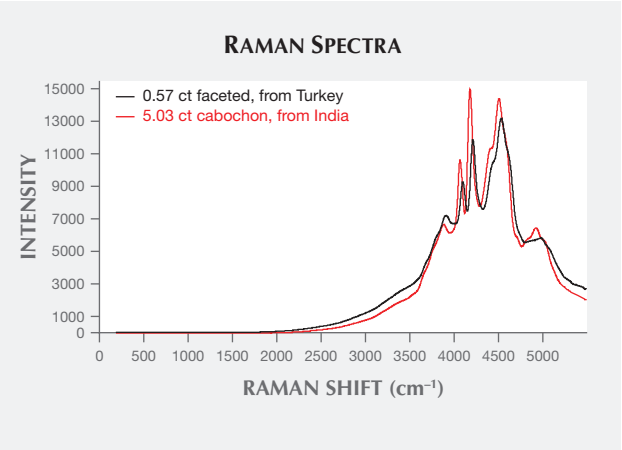

Figure 3. Raman spectra showing characteristic peaks of kämmererite at 3877, 4063, 4175, 4500, and 4920 cm^{-1}.

new massive kämmererite rough is unknown, and the material may remain rare.

Jaroslav Hyršl (hyrsl@hotmail.com)
Prague

Spectral characteristics of *Pinctada mazatlanica* and *Pinctada margaritifera* pearl oyster species. *Pinctada margaritifera* is a well-known mollusk species of the Indo-Pacific region that produces gray to black pearls. Cultured pearls from the mollusk are often referred to as "Tahitian" in the market. Both natural and cultured *P. margaritifera* pearls are noted for their characteristic UV-visible spectra. The typical reflectance feature at 700 nm is a key identification attribute for this species (K. Wada, "Spectral characteristics of pearls," *Gemmological Society of Japan,* Vol. 10, No. 4, 1983, pp. 3–11, in Japanese).

Pinctada mazatlanica, the so-called Panamanian pearl oyster, is a species closely related with *P. margaritifera*. Although *P. mazatlanica* was originally classified as a subspecies of *P. margaritifera* (R.L. Cunha et al., "Evolutionary patterns in pearl oysters of the genus Pinctada (Bivalvia: Pteriidae)," *Marine Biotechnology,* Vol. 3, No. 2, 2011, pp. 181–192), in 1961, the taxonomy of the Pinctada genus was revised, and *P. mazatlanica* was listed as a distinct species due to different shell characteristics and geographical occurrence. *P. mazatlanica* is extensively distributed along the western coast of the Americas from Mexico to Peru and around the Galapagos Islands. It is considered a native pearl oyster species of the Gulf of California in Mexico and around the Archipelago de las Perlas in the Gulf of Panama (G.F. Kunz and C.H. Stevenson, *The Book of the Pearl*, The Century Co., New York, 1908, p. 69). The spectroscopic characteristics of this species were believed to be similar to *P. margaritifera* (Winter 2005 Lab Notes, p. 347), yet this author was unable to find any recorded spectra in the literature.

GIA's Bangkok laboratory recently studied three *P. mazatlanica* shells from Mexico (two are shown in figure 4). These shells appeared to have morphology between *P. maxima* and *P. margaritifera* mollusks (P. C. Southgate and J.S. Lucas, *The Pearl Oyster,* Elsevier, Oxford, 2008, p. 60). The rounded outlines were similar to those of *P. maxima*; in each, the shell's height was almost equal to the width. The color of the outer surfaces alternated from yellowish brown to dark greenish gray, with rays of whitish blotches

Figure 4. These Pinctada mazatlanica *shells were obtained from Mexico. Left: The shell has a rounded outline, with a nearly equal height and width. The exterior surface exhibits alternating yellowish brown and dark greenish gray colors, with whitish blotches fanning out from the center. Right: The interior view of the shell on the left alongside a smaller example showing a yellowish green nacreous rim with a distinct orient. Photos by Lhapsin Nillapat.*

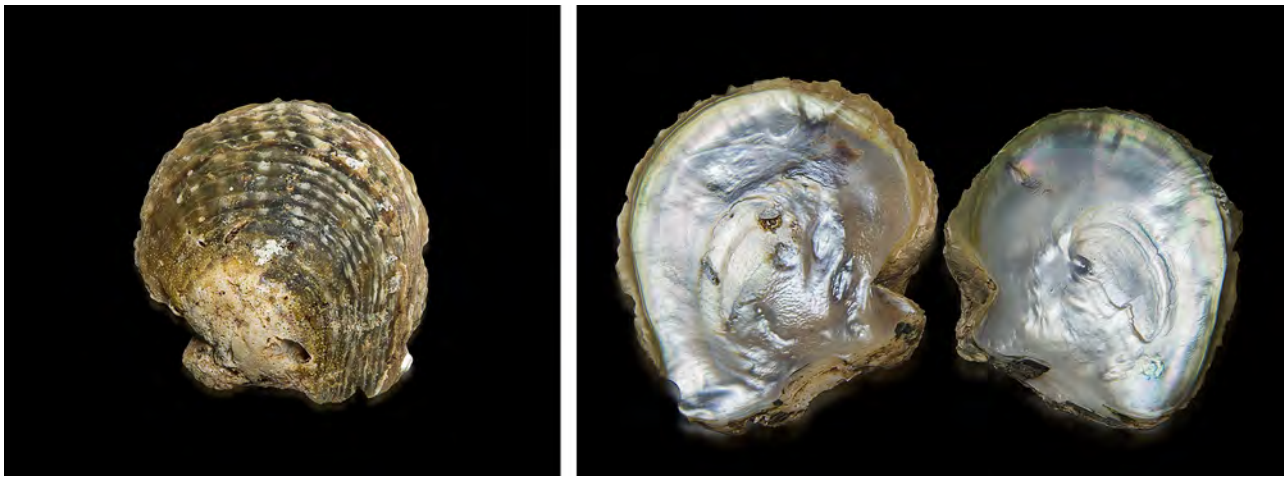

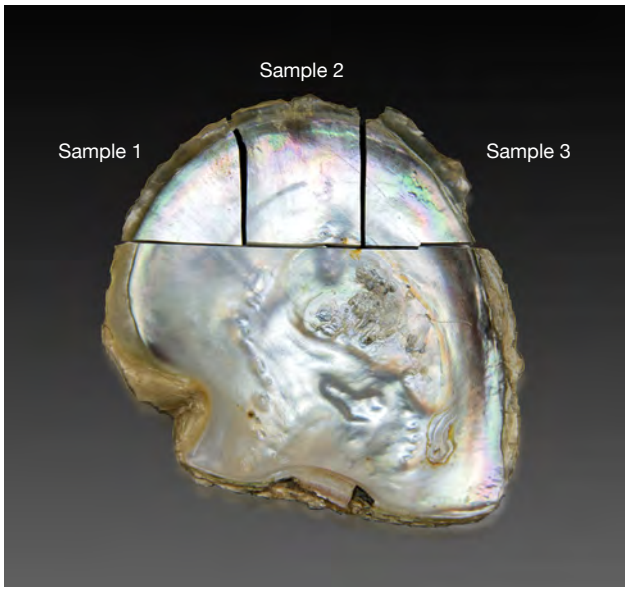

Figure 5. The lip area of one P. mazatlanica *shell was cut into three pieces to investigate the reflectance spectral characteristics in the dark and light nacreous areas. Photo by Lhapsin Nillapat.*

fanning out from the center. The inner nacreous rims ranged from yellowish green to dark gray with visibly iridescent overtones resembling *P. margaritifera*. To investigate reflectance UV-visible spectral characteristics in the dark and light nacreous areas, three pieces were cut from one of the shells (figure 5).

The dark gray nacre of all the samples exhibited the same spectral pattern as those recorded from naturally colored gray to black nacre of *P. margaritifera* shells and pearls. The reflectance feature at 700 nm was consistently present in these samples, together with a uroporphyrin feature at 405 nm (figure 6). Uroporphyrin has been established as one type of pigmentation responsible for gray to black tones in some pearl oyster species (Y. Iwahashi and S. Akamatsu, "Porphyrin pigment in black-lip pearls and its application to pearl identification," *Fisheries Science*, Vol. 60, No. 1, 1994, pp. 69–71). However, the feature at 495 nm that is often displayed in natural dark-colored nacre from *P. margaritifera* was not present in these samples, while the spectra collected in white to silver areas lacked the 405 and 700 nm characteristics. The spectra were relatively featureless, with no significant reflectance showing in the visible region. This was in keeping with results obtained from the white to silver nacre of *P. maxima* and *P. margaritifera* shells and pearls (S. Elen, "Identification of yellow cultured pearls from the black-lipped oyster *Pinctada margaritifera*," Spring 2002 *G&G*, pp. 66–72).

Further studies at GIA's New York laboratory on *P. mazatlanica* shells from GIA's Carlsbad collection confirmed these findings. Additionally, the yellow-green nacre close to the dark gray nacreous rim of the shell showed a broad trough from 330 to 460 nm. This consisted of features between 330 and 385 nm and between 385 and 460 nm. A clear feature at 700 nm was observed, but the one at 405 nm was not evident. The spectra are comparable with natural yellow *P. margaritifera* nacre samples (again, see Elen, 2002).

Photoluminescence (PL) spectra collected on the dark gray and yellow-green nacreous areas of all the samples showed bands at approximately 620, 650, and 680 nm. These same PL bands are observed in naturally colored nacre of *P. margaritifera* and *Pteria sterna*, as well as several colors of *P. maxima* nacre (S. Karampelas, "Spectral characteristics of natural-color saltwater cultured pearls from *Pinctada maxima*," Fall 2012 *G&G*, pp. 193–197).

The reflectance and PL spectra from our samples prove the close relationship between *P. mazatlanica* and *P. margaritifera*. Pearls produced by these two black-lipped oyster species therefore share similar spectral characteristics.

Artitaya Homkrajae
GIA, Carlsbad

Macedonian ruby specimens. The Macedonian town of Prilep has been a source of marble since antiquity, even supplying some Roman settlements. Rubies have occasionally been found within the Bianco Sivec quarry, according to gem dealer Denis Gravier (Gravier & Gemmes, Poncin, France). Although Prilep is mainland Europe's only known natural ruby source, only in the past 15 years has there

Figure 6. UV-visible reflectance spectra of the darker gray nacre areas of all three P. mazatlanica *shell samples shown in figure 5 are similar to the spectrum from a* P. margaritifera *pearl. All show a uroporphyrin feature at 405 nm and a feature at 700 nm, which is diagnostic of* P. margaritifera. *These spectra prove the similar spectral characteristics between* P. mazatlanica *and* P. margaritifera.

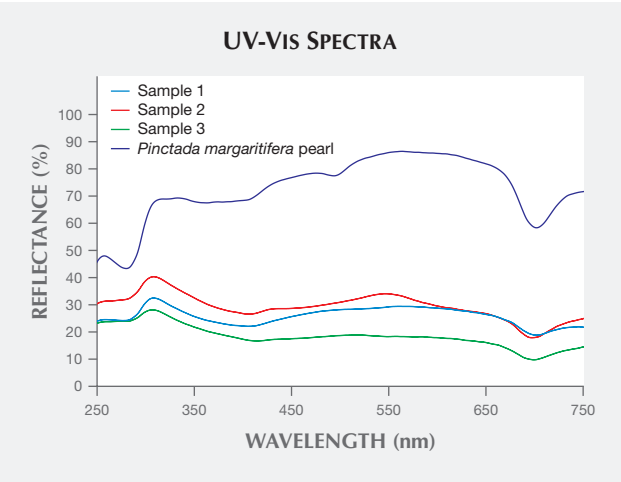

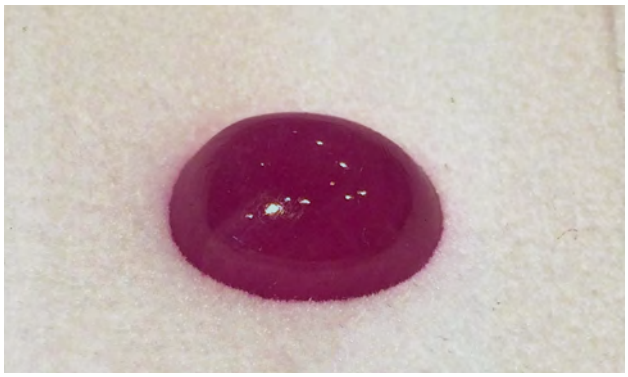

Figure 7. This 9.93 ct ruby cabochon from Macedonia was seen at the Jewellery & Gem Fair – Europe in Freiburg, Germany. Photo by Russell Shor/GIA.

been an effort to mine the gems. Gravier offered several rubies from the Prilep quarry at the March 19–22 Jewellery & Gem Fair – Europe in Freiburg, Germany, including the 9.93 ct cabochon seen in figure 7. None of the specimens were faceted. Gravier said the deposit produces comparatively few gem-quality rubies, and most are too cloudy for faceting. The best ones have a distinct "raspberry" color. It is unknown whether any of the material is heat treated. Macedonian craftsmen have developed a local industry using these rubies in jewelry and *objets d'art*.

Russell Shor
GIA, Carlsbad

Multiphase fluid inclusions in blue sapphires from the Ilmen Mountains, southern Urals. Most gem-quality sapphires are found in placers that originate from the weathering of primary deposits. Discovering a mineral *in situ*, or within the host rocks, is rare. In August 2015, some of the authors visited a corundum deposit in the Ilmen Mountains

Figure 8. Map showing the location of the blue sapphire occurrence within Russia.

Figure 9. Sapphire crystals in feldspar matrix of a syenite pegmatite from the Ilmen Mountains of Russia. The largest sapphire crystal measures 5.9 × 4.2 cm. From a private collection; photo by Elena S. Sorokina.

in the southern Urals of Russia (figure 8) to collect the stones *in situ* for research. This is a primary source where blue sapphire megacrysts are found exclusively in syenite pegmatites. The occurrence is located inside the Ilmen State Reserve, and its commercial exploitation is forbidden.

Corundum syenite pegmatites in the Ilmen Mountains present an REE-rich source of transparent to translucent blue sapphire crystals measuring up to 5.9 × 4.2 cm (figure 9). But the brittle deformation throughout the gem-bearing rocks, which appears to be linked to syntectonic and post-tectonic processes that occurred at the deposit and the surrounding area, increased the amount of fissures in the corundum. As a result, the sapphires are of a lower quality and can only be faceted into small stones. Six sapphire wafers and nine petrographic thin sections of mineral from corundum-bearing rocks of this occurrence were recently examined at GIA's Carlsbad lab.

Laser ablation–inductively couple plasma–mass spectrometry (LA-ICP-MS) and electron microprobe analysis (EPMA) indicated medium-rich Fe (2470–3620 ppmw), high Ga (190–280 ppmw), and low Mg (3–9 ppmw) with Ga/Mg > 29, all in the range of magmatic sapphires (see J.J. Peucat et al., "Ga/Mg ratio as a new geochemical tool to differentiate magmatic from metamorphic blue sapphires," *Lithos*, Vol. 98, No. 1–4, 2007, pp. 261–274).

Ferrocolumbite, zircon, and alkali feldspar group minerals, identified by confocal micro-Raman spectroscopy, were observed as syngenetic inclusions. Epigenetic muscovite and exsolved needles (most likely ilmenite) were found as well; along with syngenetic inclusions, they are

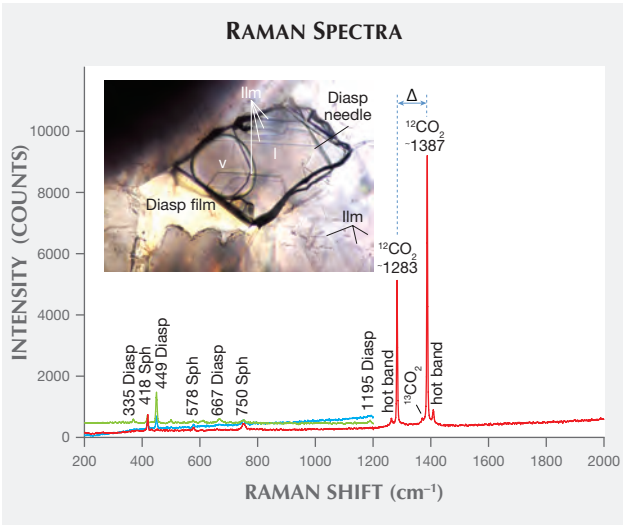

Figure 10. Raman spectra at room temperature of a fluid inclusion trapped in a sapphire from the Ilmen Mountains: $^{12}CO_2$ Fermi doublet along with hot bands and $^{13}CO_2$ peak (red trace), diaspore needle (blue), and a diaspore thin film (green). For $^{12}CO_2$, the average distance between Fermi doublet peaks (Δ) was calculated as 104.25 cm^{-1}. Diasp = diaspore, Sph = sapphire, Ilm = ilmenite, l = liquid CO_2, v = vapor CO_2. Photomicrograph by Elena S. Sorokina; polarized transmitted light, field of view 0.288 mm.

common phases in mineral assemblages of Ilmen corundum syenite pegmatites (see V. F. Zhdanov et al., "The mineralogy of corundum pegmatite pit no. 298 of the Ilmen State Reserve," *Materialy k mineralogii Yuzhnogo Urala* [*Materials to Mineralogy of South Urals*], AS USSR, 1978, pp. 92–97, in Russian). Wafers 200–400 µm in width were prepared in order to study fluid inclusions (FI) trapped within the sapphire crystals.

Using Raman spectroscopy, solid phases in needle and thin-film form were identified as diaspore (figure 10); both vapor and liquid phases were found to be CO_2, with a Fermi doublet for the liquid phase at 1282.9–1283.2 and 1387.2–1387.6 cm^{-1}, accompanied by less intense symmetrical bands ("hot bands"; see N.B. Colthup et al., *Introduction to Infrared and Raman Spectroscopy*, 2nd ed., Academic Press, New York, 1975) at approximately 1264 and 1408 cm^{-1} and a small band at 1370 cm^{-1} due to $^{13}CO_2$. Raman spectra in the 2000–4000 cm^{-1} range did not show H_2O-, CH_4-, or N_2-related bands. The less intense apparent maxima at 418, 578, and 750 cm^{-1} belong to sapphire vibration modes. The distance between Fermi doublet peaks (Δ) ranged from 104.1 to 104.4 cm^{-1} (again, see figure 10), occurring at about 0.7 g/cm^3 CO_2 density (see X. Wang et al., "Raman spectroscopic measurements of CO_2 density: Experimental calibration with high-pressure optical cell (HPOC) and fused silica capillary capsule (FSCC) with application to fluid inclusion observations," *Geochimica et Cosmochimica Acta*, Vol. 75, 2011, pp. 4080–4093). The distance was linked to the pressure at approximately 1.8 kbar for the trapping of fluid inclusions within the sapphire matrix (CO_2 P-T *isochores*, or lines of constant density). The CO_2 homogenization temperature (the temperature at which the fluid inclusion becomes a single-phase liquid or vapor) occurred in the liquid phase and measured between 30.1° and 30.7°C (figure 11), while the corundum-diaspore equilibrium was estimated at 510°–530°C (matching the previous estimation by V.A. Simonov, *Usloviya mineraloobrazovaniya v granitnykh peg-*

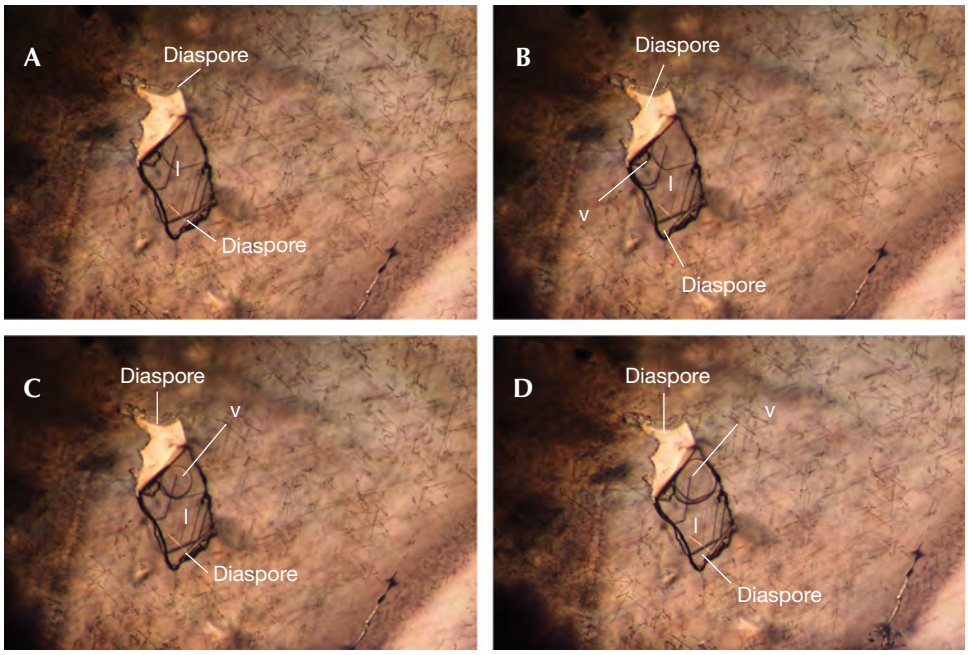

Figure 11. Homogenization of CO_2 in a fluid inclusion in sapphire from the Ilmen Mountains occurs in the liquid phase between 30.1° and 30.7°C. A: Homogenization of CO_2 above 30.7°C. B and C: Vaporization of CO_2 with a temperature below 30.7–30.1°C. D: The multiphase FI at room temperature. l = liquid, v = vapor. Photomicrographs by Jonathan Muyal; transmitted polarized illumination, field of view 0.72 mm.

matitakh [*Conditions of Mineral Formation in Non-Granitic Pegmatites*], Nauka, Novosibirsk, USSR, 1981, in Russian). Based on the determined pressure (around 1.8 kbar), the temperature of stability for the corundum-orthoclase-H_2O system was higher than 690°C (H.S. Yoder and H.P. Eugster, "Synthetic and natural muscovites," *Geochimica et Cosmochimica Acta*, Vol. 8, 1955, pp. 225–280), likely linked to the multistage geological history of blue sapphire crystallization along the P-T path in the Ilmen Mountains.

Further study of these sapphires is needed to better understand the geological history of this locality, but the information obtained can provide valuable clues about the characterization of gem corundum from secondary placers.

Elena S. Sorokina (elena.sorokina@gia.edu)
GIA, Carlsbad
Fersman Mineralogical Museum RAS, Moscow
John I. Koivula and Jonathan Muyal
GIA, Carlsbad
Stefanos Karampelas
Gem Research Swisslab AG (GRS)
Adligenswil, Switzerland
Tursun P. Nishanbaev and Sergey N. Nikandrov
Ilmen State Reserve, Miass, Russia

Tremolite and diopside bead with unusual texture and color. In recent years, Buddhist prayer beads have become increasingly popular in Chinese jewelry. These beads are made into a variety of shapes from many kinds of gem materials.

At the 2015 China International Jewelry Fair in Beijing, a barrel-shaped bead with unusual green and white color (figure 12) attracted our interest. The bead weighed 6.39 g and measured approximately 30.5 × 10.8 × 10.5 mm. The hydrostatic specific gravity (SG) was 3.05, but it was difficult to obtain individual spot RIs from the white and green areas. The entire sample was inert to both long-wave and short-wave UV. The infrared reflectance spectrum (figure 13) of the whitish mineral indicated tremolite, with characteristic peaks at 1093, 988, 902, 743, 676, 529, and 470 cm^{-1}, while the greenish mineral's spectrum matched that of diopside, with peaks at 1060, 979, 921, 681, 511, and 410 cm^{-1}.

Figure 12. This 6.39 gram barrel-shaped bead was unusual for its texture and color. Photo by Yanjun Song.

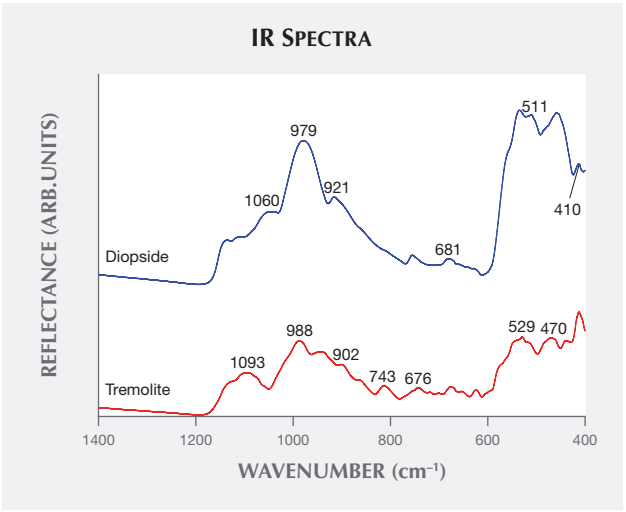

Figure 13. IR spectroscopy identified the whitish mineral in the bead as tremolite (red trace, peaks at 1093, 988, 902, 743, 676, 529, and 470 cm^{-1}) and the greenish one as diopside (blue trace, peaks at 1060, 979, 921, 681, 511, and 410 cm^{-1}). The spectra are offset for clarity.

Raman spectra of the white and green areas (figure 14) were obtained using 785 and 532 nm laser excitation, respectively. Peaks at about 1058, 1028, 754, 673, 394, and 224 cm^{-1} indicated tremolite, while those at 1013, 667, 559, 393, and 326 cm^{-1} were consistent with diopside.

Tremolite and diopside are common gem materials in the jewelry trade. Both occur in nephrite, where tremolite is the main mineral and diopside is an accessory mineral. This was the first time we had encountered diopside rather than tremolite as the major mineral when both occurred within the same sample.

Yanjun Song
Earth Science and Resources College
Chang'an University, Xi'an, China
Yungui Liu
College of Gemstone and Material Technology
Shijiazhuang University of Economics, China
Xiaoqiang Xia
Beijing Institute of Gemology
Juan Zhao
Xi'an Center of Geological Survey (CGS), China

SYNTHETICS

Synthetic moissanite imitations of synthetic colored diamonds. Three faceted specimens were recently submitted to the Earth Science and Resources College of Chang'an

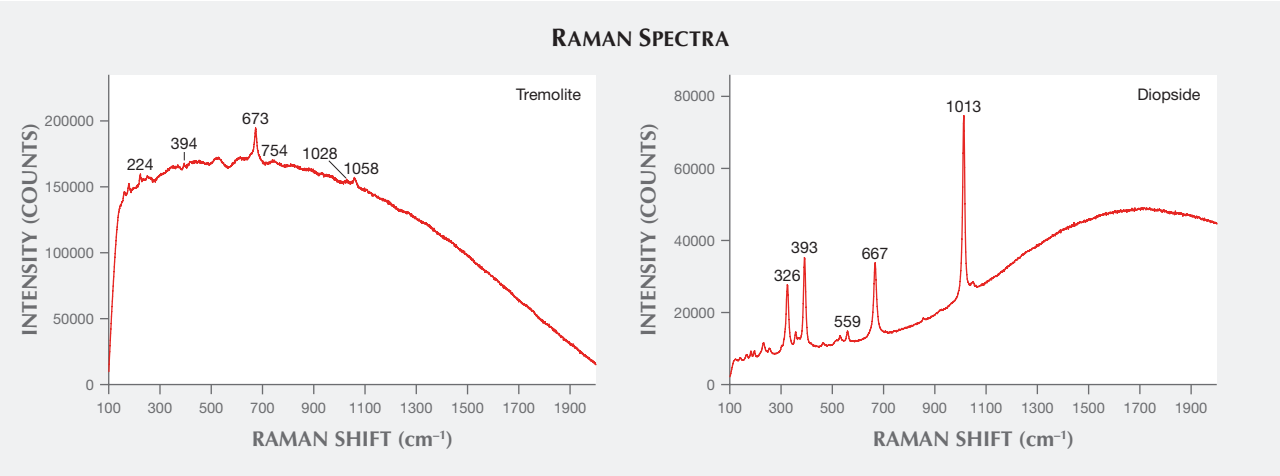

Figure 14. Raman spectra of the barrel-shaped bead. Left: Peaks at 224. 394, 673, 754, 1028, and 1058 cm^{-1} were indicative of tremolite. Right: Peaks at 326, 393, 559, 667, and 1013 cm^{-1} were consistent with diopside.

University by a client who acquired them as synthetic colored diamonds (figure 15). All three specimens were relatively clean to the unaided eye. The RI of the specimens was over the limit of the gem refractometer. The average hydrostatic SG value was 3.21, and all samples were inert under long-wave and short-wave UV radiation. Microscopic examination revealed clear doubling of numerous stringers and some needle-like inclusions (figure 16). All of these features were consistent with synthetic moissanite (K. Nassau et al., "Synthetic moissanite: A new diamond substitute," Winter 1997 *G&G*, pp. 260–275). Raman spectra of the samples were obtained using 785 nm laser excitation from three different orientations: parallel to the c-axis, perpendicular to the c-axis, and random orientation (one specimen's spectra is shown in figure 17). Results for all three samples indicated synthetic moissanite, with the peaks at 149, 767, 789, and 967 cm^{-1} obtained from the random orientation (see rruff.info).

Moissanite (silicon carbide, or SiC) has many polytype structures, including cubic (C), hexagonal (H), and rhom-

Figure 15. Submitted as synthetic diamonds, the 0.99 ct blue-green emerald step cut (left), 0.85 ct brown-yellow standard round brilliant (center), and 1.90 ct deep green standard round brilliant (right) were all identified as synthetic moissanite. Photo by Yanjun Song.

Figure 16. Needle-like inclusions (top) and doubling of numerous stringers (bottom) are shown here in the emerald step cut. Photomicrographs by Yanjun Song; field of view 4.22 mm (top) and 2.26 mm (bottom).

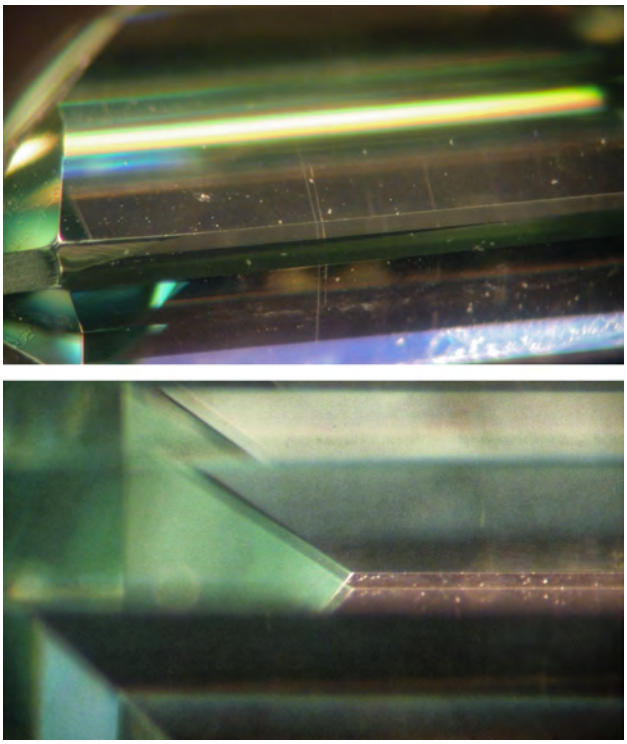

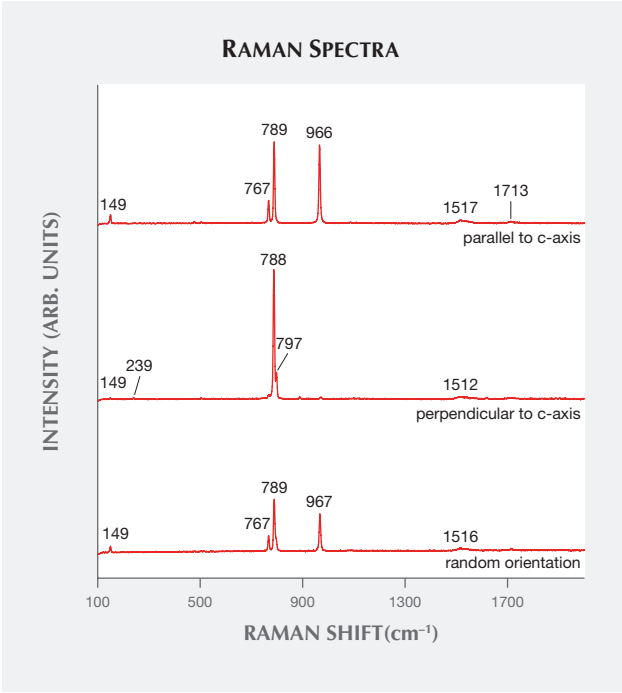

Figure 17. Raman analysis of the emerald step cut from three different optical orientations, using a near-infrared wavelength of 785 nm, confirmed its identity as synthetic moissanite.

bohedral (R). Hexagonal structure 4H-SiC and 6H-SiC (space group P63mc) are the most common polytypes used as gem material. In this study, the characteristic peaks at 149, 767, 789, and 966 cm^{-1}, obtained from the orientation parallel to the c-axis, were consistent with those previously reported for 6H-SiC (S. Nakashima and H. Harima, "Raman investigation of SiC polytypes," *Physica Status Solidi A*, Vol. 162, No. 1, 1997, pp. 39–64).

High-quality colorless and black synthetic moissanites are common diamond imitations in the jewelry trade. As the growth techniques of synthetic moissanite continue to improve and the popularity of fancy-color diamonds increases in the Chinese market, we anticipate that high-quality synthetic colored moissanite will become more prevalent.

Yanjun Song

Lu Zhang
Institute of Prospecting Technology
Hebei Mine Bureau, Langfang, China

Yunlong Wu
National Testing Center for Gold and Silver Jewelry
Tianjin, China

TREATMENTS

Steam-dyed amber. "Beeswax" amber, a common trade name used in the Chinese gem market, refers to yellow amber that has a semitranslucent, opalescent, milky appearance with greasy luster. Among the beeswax ambers, "chicken-fat yellow beeswax" is very popular for its bright color. Global production is limited, and the material is in high demand in the Chinese amber market. Therefore, many methods to enhance the color of beeswax amber have been attempted. In March 2016, the Guangzhou laboratory of the Gem Testing Center, China University of Geosciences (Wuhan) received four pieces of chicken-fat yellow beeswax amber samples from two different clients (figure 18); two more pieces were received in May from an unrelated owner (figure 19).

Infrared spectroscopy showed all ambers with typical "Baltic shoulder" patterns in the 1100–1300 cm^{-1} range, with low and broad bands in higher frequencies and a high, sharp peak at 1160 cm^{-1}. Instead of the whitish yellow of natural Baltic ambers, we saw either bright yellow or orange hues, both of which are unusual. Under strong transmitted light, the yellow color of the round bead in figure 18 (left) showed a mottled distribution, which was proof of

Figure 18. Left: This "chicken-fat yellow beeswax" amber bead, approximately 15 mm in diameter, was treated by the steam dyeing method. Right: The unusually dark orange color of these pear-shaped samples comes from steam dyeing. Photos by Fen Liu.

Figure 19. The two bright yellow beads in the center, 8 mm and 9 mm in diameter, were treated by steam dyeing, while the bracelet contains natural-color amber. Photo by Jiewan Huang.

Figure 20. The darker mottled color patches in this sample indicate that the bead was unevenly dyed. Photo by Fen Liu.

uneven dyeing (figure 20); however, microscopic examination revealed small squashed bubbles caused by "steam treatment." Further, red color filaments unrelated to the cracks among the bubbles near the surface were traces of residual dyes (figure 21, left).

The color of the pear-shaped samples appeared to be darker than the yellow associated with chicken-fat amber (again, see figure 18, right). This darker color faded slightly when the surface was swabbed with alcohol. Under 40× magnification, the bubbles appear to have yellow meniscuses. The bubble-rich regions were darker than the portions with fewer bubbles. In some areas among the bubbles, an abnormal dark orange color zone appeared to be induced by residual color matter (figure 21, right). All these observations indicated the amber pieces underwent some artificial treatment. The clients admitted that these beeswax ambers were treated by a new treatment method, called "steam dyeing," which delivers gas bubbles from colored water into the amber structure at pressure and temperature conditions close to those of saturated water vapors.

Steam dyeing treatment is easy to miss. The rapid development in amber treatment methods means that con-

Figure 21. Left: The squashed bubbles are induced by steam treatment, and the red filaments are possible traces of residual dye. Photomicrograph by Fen Liu; field of view 2.95 mm. Right: The dark orange color zone among the bubbles, unrelated to the cracks, indicates that the color zone was introduced by dyeing. Photomicrograph by Shufang Nie; field of view 2.95 mm.

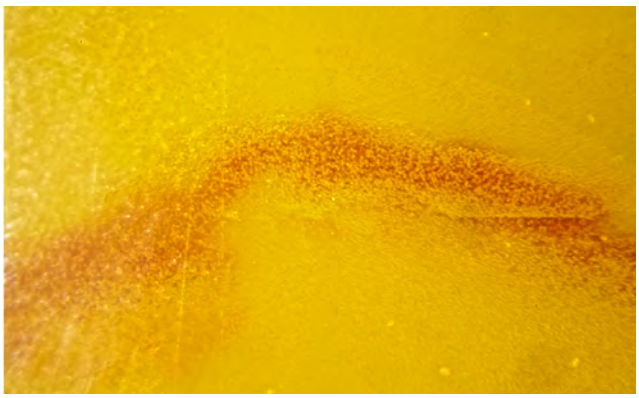

sumers and laboratories must be cautious when dealing with these "chicken-fat yellow beeswax" ambers.

Yamei Wang, Fen Liu, Shufang Nie, and Andy Shen
Gem Testing Center, China University of Geosciences (Wuhan)

Polymer-coated serpentine. Jadeite, nephrite, serpentine, chalcedony, and quartzite were all referred to as "jade" in ancient China, where objects were defined by their craftsmanship rather than the materials themselves. The term is still widely used in the Chinese market for many types of materials. "Xiuyan jade" is actually a form of serpentine, so named for Xiuyan, a city in China's Liaoning province where serpentine deposits are abundant.

The pendant in figure 22 was submitted to the Lai Tai-An Gem Laboratory by a client who claimed the material was jadeite jade. The pendant, which weighed 222.03 ct and measured 58 × 37 × 17 mm, showed a light green carved fish on a brown and yellow background. At first glance, it appeared to display a plastic-like luster.

Identical spot RIs of 1.56 were obtained from two different parts of the object, and an SG of 2.40 was determined. Both measurements were lower than expected for jadeite. The SG may have been affected by a polymer coating; this was partially confirmed when bubbles were observed on some surface areas under magnification. Microscopic observation proved that the piece was solid and not assembled. It was inert under long-wave and short-wave UV light from an ultraviolet viewing cabinet, whereas most polymer-coated objects show weak to strong reactions. The client granted permission to cut the piece in two for further analysis.

DiamondView observations of the cross section revealed an inert reaction from the object's interior, but the coatings on the surface produced a strong bluish fluorescence (figure 23). FTIR spectroscopy on the interior identified the material as serpentine, but peaks at 3060, 3025, 2932, and 2858 cm^{-1}, obtained from the surface, showed that a polymer was present. Peaks at 1045, 673, 564, and 485 cm^{-1}, detected from both the interior and the surface, were indicative of serpentine (figure 24); this was confirmed by Raman spectroscopy.

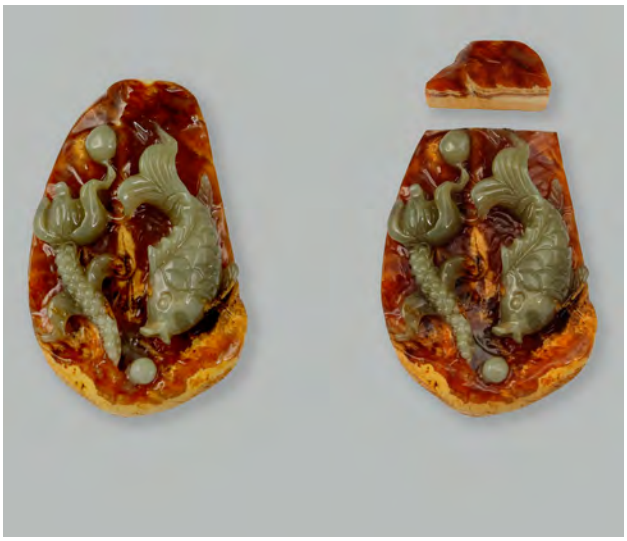

Figure 22. The serpentine pendant before and after cutting. Photos by Lai Tai-An Gem Lab.

Coatings are normally applied to gem materials to improve luster and, in some cases, provide a degree of stability. This was the first case of coated serpentine we have encountered. Care should be taken to identify such coatings; the simplest way to detect the treatment is to check for any unusual reaction under the ultraviolet viewing cabinet, but in this case, the UV reaction only showed in the ultra-short-wave UV of the DiamondView. Serpentine's characteristically low hardness makes it a very suitable carving material, but any treatments applied to it should be fully disclosed.

Larry Tai-An Lai (service@laitaian.com.tw)
Lai Tai-An Gem Laboratory, Taipei

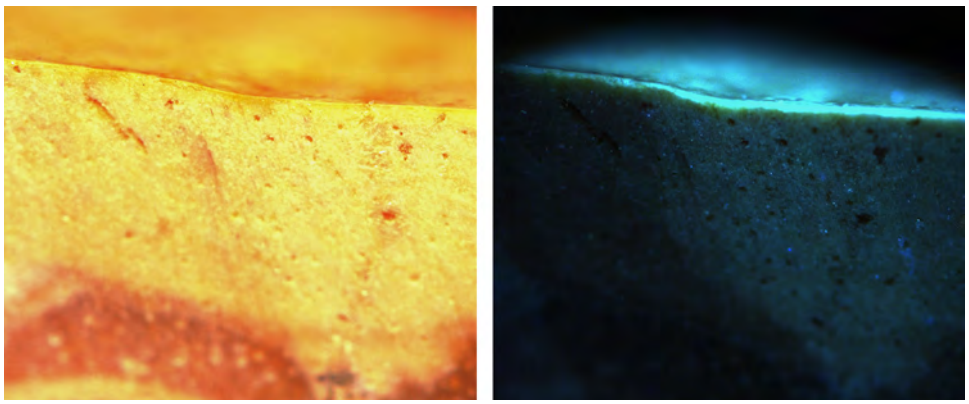

Figure 23. DiamondView imaging showed that the inner portion of the serpentine was inert, while the surface exhibited a strong bluish fluorescence. These images show the reflection from the polymer-coated surface in visible (left) and UV light (right). Images by Lai Tai-An Gem Lab.

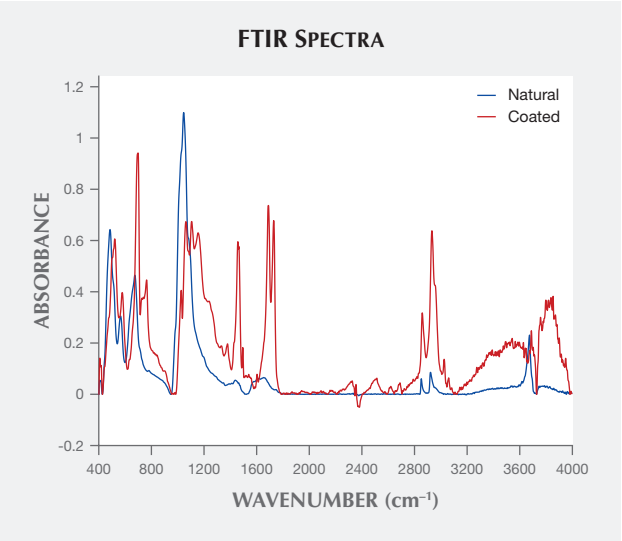

Figure 24. FTIR spectroscopy revealed peaks indicative of coating at 2858, 2932, 3025, and 3060 cm^{-1} (red) and serpentine peaks at 485, 564, 673, and 1045 cm^{-1} (blue).

MORE FROM TUCSON

Almandine in graphite schist specimens. At this year's Tucson shows, the authors saw the breathtaking almandine-pyrope in graphite schist specimens that debuted at the August 2014 East Coast Gem, Mineral, and Fossil Show in Springfield, Massachusetts (figure 25). Mine owner Jason Baskin (Jay's Minerals, Flemington, New Jersey) first encountered the material from the Red Embers mine (then called the Two Fat Guys mine) in Franklin County, Massachusetts, in the early 2000s, and his family bought the mineral rights to this property in 2008. Mr. Baskin, along with his cousin Kyle Baskin and uncle Kevin Baskin, worked the mine (currently closed to the public) by hand, with tools such as chisels and hammers, for six years before unveiling these specimens and the location of the mine (figure 26).

Good-quality almandine specimens are found in various localities in the eastern United States. This deposit is located in a metamorphosed zone full of layered graphite schist. According to Mr. Baskin, the thickness of the veins can vary from about 1 to 6 feet wide. Black columnar accompanying minerals can be found in the graphite matrix in between the garnet crystals on some specimens (figure 27). This long needle-like mineral was identified as dravite tourmaline. Based on his many years of mining experience at this location, Mr. Baskin says that the garnet crystals tend to have higher quality when they occur within a fold. Some of the garnet crystals are suitable for faceting, but it is the specimens that generate the most purchases. The largest crystal found to date is 28 mm in diameter; the largest faceted stone is 4.7 ct.

Figure 25. Jason Baskin is seen holding his largest almandine in graphite schist specimen at the 2014 Springfield Mineral Show. This specimen is now part of the collection of the Mineralogical and Geological Museum at Harvard University. Photo courtesy of Jay's Minerals.

These striking specimens displayed sharp, dark red trapezohedra in fine-grained silvery graphitic schist (R.B.

Figure 26. Jason Baskin displays two giant pieces of graphite schist extracted from the mine. Hand tools such as the sledgehammer behind him are used to mine the specimens. Photo courtesy of Jay's Minerals.

Figure 27. With a strong light source behind the specimen, the garnet crystals within the graphite glow, showing an attractive burgundy color. The black columnar mineral in the graphite matrix was identified as dravite. Not all specimens contain dravite, though its presence adds charm to the piece. Photo courtesy of Jay's Minerals.

Cook, "Almandine New York City, New York County, New York State," *Rocks & Minerals*, Vol. 84, No. 3, 2009, pp. 244–252). In a previously published article, Raman spectroscopy identified the garnet as predominantly almandine with some spessartine and minor pyrope components (C. Williams and B. Williams, "Almandine from Erving, Massachusetts," *Journal of Gemmology*, Vol. 34, No. 4, 2014, pp. 286–287). Most specimens have multiple garnet crystals embedded in them, with the largest containing more than 100 crystals.

Due to the fine-grained nature of the host rock, a dust mask must be worn during the mining process. The most attractive aspect of these specimens is the exposure of the garnet crystals from both sides of the rock, which allows the light to travel through and make the garnet glow, showing its deep burgundy color (again, see figure 27). To achieve this goal, Baskin has tried numerous abrasives to remove the schist on both sides of the garnet without affecting the crystals' surfaces. Some of the experimental abrasives included various kinds of glass beads, plastic beads, corn cobs, and even walnut shells. Finally, a special plastic made it possible to expose the garnets from both sides efficiently. The Mineralogical and Geological Museum at Harvard University, the American Museum of Natural History, Yale University, the University of Arizona, and Bill Larson of Pala International all currently own these specimens.

Tao Hsu and Andrew Lucas
GIA, Carlsbad

Australian opal beads with blue play-of-color. The Australian Opal Shop (Gold Coast, Australia) had a variety of goods on display at Tucson's Globe-X Gem & Mineral Show. Owner John McDonald primarily deals in boulder opal with a sandstone matrix from the Winton mining area in Queensland. Untreated specimens can be polished to create beautiful slabs of boulder opal with or without matrix, though sandstone with microscopic bits of opal must be treated to make the play-of-color visible. The pieces are soaked in a fatty oil (usually vegetable oil) rather than petroleum-based oils, which leave a residue. The finished product ranges from multicolored to dark blue, depending on the size of the opal pockets and the spherical structure. What appears as dark blue bodycolor is actually blue play-of-color. The treated rough is usually fashioned into beads (figure 28).

Donna Beaton
GIA, New York

Honduran and Turkish opal. Harald Mühlinghaus (Opal Imperium, Enkirch, Germany) has been exhibiting at the Pueblo Gem & Mineral Show for more than 20 years. The company sources, fabricates, and sells a number of colored gemstones, but their main focus is opal from Australia, Mexico, Honduras, and other locales. At the booth were some unusual examples that have rarely been documented, such as a banded opal (figure 29, left) obtained about 30 years ago from an unrecorded Honduran location. This material occurs as solid vertical veins in matrix with approximately 1 cm stratifications of play-of-color, which indicate the cyclical concentration and the formation of the silica spheres that form opal. The phenomenon is most distinct in fairly sizable pieces of rough, with 1–3 mm opal layers

Figure 28. At the Globe-X show, these polished Australian opal beads (in sandstone matrix) displayed blue play-of-color. Photo by Donna Beaton.

Figure 29. Left: This Honduran banded opal, 10 cm in height, shows a 1–3 mm thick stratified opal layer attached to matrix. Right: Turkish dendritic opal was available as cabochons. Photos by Donna Beaton.

on matrix measuring 5–15 cm across, which makes these specimens more suitable for display than for jewelry. Some of the smaller examples displayed only nonphenomenal layers, while others had play-of-color fading to potch at each cycle.

Also on display were dendritic opal cabochons (figure 29, right) from rough obtained from Simav, Turkey, about four years ago. This material, which Mühlinghaus called "Turkish dendritic opal," has been cut so that each piece shows clearly delineated opaque white and semitransparent areas, embedded with fine branched black inclusions reminiscent of traditional Japanese *tategaki* characters.

Donna Beaton

African rhodochrosite and Colombian quartz with trapiche patterns. Also at the Pueblo show, Germán Salazar (Idar-Oberstein and Bogotá) and Gaetano Lacagnina (L.G. Gemme, Milan) shared a booth that featured an eclectic assortment of gems and minerals. Mr. Lacagnina, who also operates a lab and cutting factory, specializes in unusual and fine mineral specimens. Of particular note were high-quality rhodochrosites from the N'Chwaning mining area in the Northern Cape province of South Africa (figure 30, left). N'Chwaning, noted for having Africa's largest manganese reserves, also produces manganite, ettringite, and other Mn-bearing minerals. Noteworthy on Mr. Salazar's side of the booth were polished hexagonal quartz slices bearing a spoked trapiche-like pattern (figure 30, right). Coincidentally, the quartz was from the Boyacá region of Colombia, which regularly produces trapiche emerald. The patterned areas are found at the core of larger quartz crystals. Viewed in a polariscope, the growth directions and fibrous inclusions are very distinct. Although Mr. Salazar has marketed the slices as "trapiche quartz," he is considering branding this unique find as "Salazarite."

Donna Beaton

The fluid art of Angela Conty. Renowned lapidary, designer, and goldsmith Angela Conty created a jewelry collection exclusively for the 2016 Tucson gem and mineral shows. We had a chance to see some of her convertible pieces at the Hotel Tucson City Center.

Ms. Conty's artistic vision is heavily influenced by nature: Flowers, leaves, twigs, seed pods, and similar motifs

Figure 30. Left: A 6.0 cm tall rhodochrosite specimen from the N'Chwaning mining area in South Africa. Right: These domed hexagonal quartz slices from Colombia, measuring 3.5–4.5 cm across, exhibit inclusions reminiscent of trapiche emerald. The pattern becomes more distinct when viewed through cross-polarized filters. Photos by Donna Beaton.

Figure 31. This pin/pendant features two Oregon sunstones, a Chinese freshwater pearl, and diamond accents. Carved green chalcedony and a 1.50 ct zircon complete the design. The piece is set in 14K and 18K yellow gold. Photo by Robert Weldon/GIA; courtesy of Angela Conty.

Figure 32. This 18K yellow gold convertible pendant/pin features a 46.80 ct carved Oregon sunstone as its centerpiece. A chocolate Tahitian pearl drop and diamond accents help frame the carving. Photo by Robert Weldon/GIA; courtesy of Angela Conty.

are reflected in her work. The fluidity of her artistic expression strikes a perfect balance and flow between the gemstone carving and the jewelry design. Ms. Conty views her design and manufacturing process as the evolution of a work of art that often features a carved gemstone. Changes may occur when carving the stone, working the metal, or assembling the piece of art. When she has the rough in hand, she takes into consideration the stone's shape, its best orientation, and how it would look carved and set in jewelry. As the carving progresses, the rough might take an unexpected direction, even after the metalwork is finished. She feels that lapidary work and metalsmithing must blend and harmonize in order to create the perfect balance. This means the carving or the metalwork can be continually adjusted until the carving is ready to be set. In her words, "I gather together elements, cast and constructed, and begin to solder or weld until the carving, gemstones and metalwork begin to work together, always ready to make more changes. I add, move, and remove elements to create a better integration of carving and goldwork."

Her gemstone preferences include Australian opal, quartz, chalcedony, and her new favorite, Oregon sunstone. Her metal of choice is 18K gold, but she will sometimes use silver or 14K gold, depending on the design or the client's preference. The relationship between the stone and metal is beautifully demonstrated in the Oregon sunstone jewelry pieces shown in figures 31 and 32, which can be worn as either brooch or pendant.

Ms. Conty's combined talents in art and creative design took root more than 40 years ago at the State University of New York (SUNY) at New Paltz, where she earned undergraduate and graduate degrees in art. Her training included drawing, art history, painting, ceramics, sculpture, and silversmithing. She studied metalwork under Kurt Matzdorff, the founder of the Society of North American Goldsmiths (SNAG), and is a self-taught lapidary artist.

In 2002, Ms. Conty won second place in AGTA's Cutting Edge Awards in the Objects of Art category. Her work has been featured in numerous publications and books.

Carl Chilstrom and Sharon Bohannon
GIA, Carlsbad

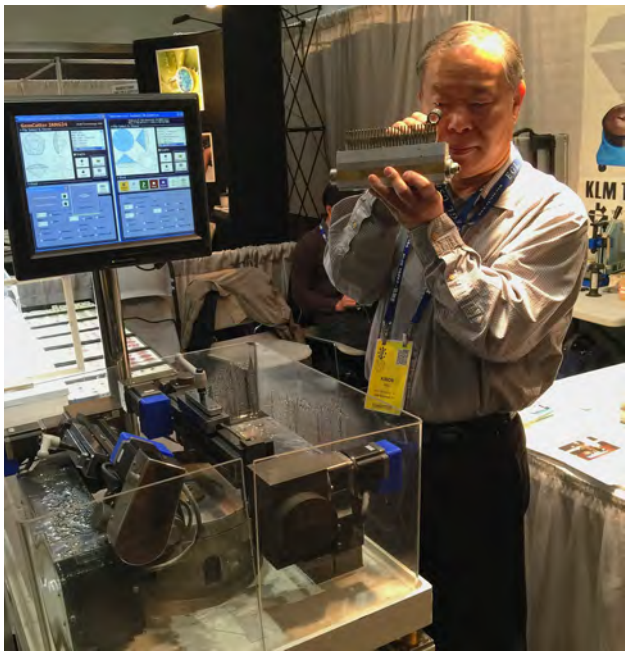

Figure 33. Kiwon Jang checks a cassette of stones during the Jang 1024's robotic cutting process. Photo by Tao Hsu.

Robotic colored stone cutting machines. At the technology pavilion of the AGTA show, master cutter Kiwon Jang of KLM Technology (New Brunswick, New Jersey) demonstrated the Jang 1024, a robotic system for cutting colored stones (figure 33).

Figure 34. A cassette of stones is cut using water as a cooling agent. Photo by Tao Hsu.

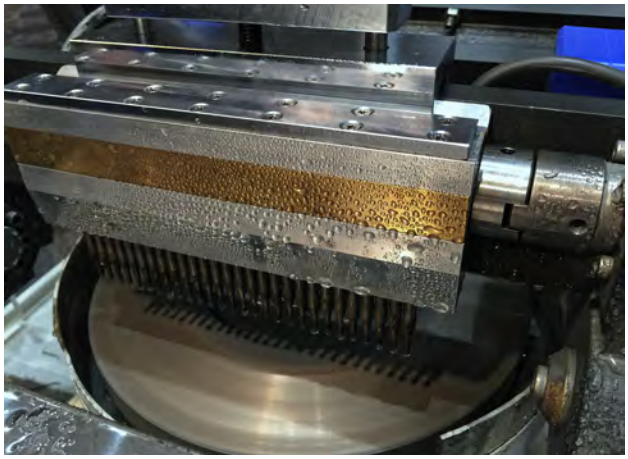

Figure 35. This cassette, which can hold up to 56 melee at one time, is shown holding 28 larger stones. Photo by Tao Hsu.

KLM provides cutting services to the gem trade. Mr. Jang began his career working with cubic zirconia in his native Korea. Since moving to the United States 30 years ago, he has developed multiple systems for automatic gem cutting, with 10 systems in KLM's New Jersey factory. The company also sells the machine to overseas clients and provides on-site training for the systems. *G&G* previously reported on one of his compact machines (Fall 2012 GNI, p. 233).

The Jang 1024 is his most recent product. The machine's process is controlled by a computer installed with designing and cutting software written by Mr. Jang. The water-cooled system (figure 34) is designed for mass production; depending on stone size, it can handle up to 56 melee at a time (figure 35). The machine can produce a round brilliant cut from 1 to 30 mm, while the largest size for emerald cuts is 25 mm. According to Mr. Jang, the maximum tolerance the machine can accommodate is 0.05 mm. The daily capacity of this machine is 2,000–4,000 melee between 1.0 and 3.0 mm, 400–800 stones between 3.5 and 10.0 mm, or 100–200 stones larger than 10.0 mm. Aside from periodically checking the stones, the entire process from preforming to polishing is done by the computer. Mr. Jang informed us that the majority of his clients are miners and cutting factories in Brazil and Russia, along with many African countries. Most of his customers in the United States are domestic dealers seeking fast local service.

Tao Hsu and Andrew Lucas

ERRATUM

In the Spring 2016 Lab Note on the largest blue HPHT synthetic diamond examined to date, the DiamondView images showing fluorescence and phosphorescence (p. 74) were listed in the wrong order.